Oil Shale, 2012, Vol. 29, No. 4, pp. 306–321
doi: 10.3176/oil.2012.4.02
ISSN 0208-189X

SOURCE REGIONS AND THE SEDIMENTARY PALEOENVIRONMENT OF MARINE OIL SHALE FROM THE BILONG CO AREA, NORTHERN TIBET, CHINA: AN SR-ND ISOTOPIC STUDY

XIUGEN FU*, JIAN WANG, YUHONG ZENG, FUWEN TAN, XINGLEI FENG

Chengdu Institute of Geology and Mineral Resources, Chengdu 610081, China

Abstract. *The Bilong Co oil shale zone is located in the South Qiangtang depression, northern Tibet, southwestern China. This zone, together with the Shengli River-Changshe Mountain oil shale zone in the North Qiangtang depression, northern Tibetan Plateau, potentially represents the largest marine oil shale resource in China. Altogether 18 samples of oil shale and micritic limestone were collected from the Bilong Co area to determine their Sr and Nd isotopic composition, as well as discuss sediment sources and paleoenvironmental changes. The Sm-Nd model ages for the Bilong Co oil shale samples support its derivation from the Nadi Kangra source whose model ages reflect the origin of volcanic rocks from the older continental crust by its melting. The Nd isotopic composition of the Bilong Co oil shale is similar to that of Late Triassic Nadi Kangri Formation volcanic-volcaniclastic rocks, which implies that this oil shale stems from said rocks.*

Generally, the vertical variations of $\varepsilon_{Nd}(0)$ values in the Bilong Co oil shale section are relatively homogeneous, suggesting a stable provenance for sediments.

The $^{87}Sr/^{86}Sr$ ratio of the Bilong Co oil shale is much higher than that of contemporary seawater. Such a high $^{87}Sr/^{86}Sr$ ratio reflects the original composition of the deposited sediment, both chemical and clastic. In the Bilong Co oil shale area, micritic limestone generally has a slightly lower $^{87}Sr/^{86}Sr$ ratio than oil shale. The Sr isotopic fluctuation in the Bilong Co oil shale is closely connected with sea level change. Sea level rise and consequent marine incursion may change the aquatic environment of the pre-existing lagoon, lowering the $^{87}Sr/^{86}Sr$ ratio of the precipitation fluid.

Keywords**:** *marine oil shale, Sr-Nd isotope, source region, paleoenvironmental change, Qiangtang basin, northern Tibet, China.*

* Corresponding author: e-mail *fuxiugen@126.com*

1. Introduction

In China oil shale as an alternative energy resource has received much attention in recent years [1, 2]. Chinese oil shale was mainly deposited in lacustrine environments. Examples are the Tertiary oil shale in the Huadian [2] and Fushun areas [1], and the Jurassic oil shale in the Minhe basin [3]. Marine oil shale is mainly found in the Qiangtang basin, northern Tibet, China [4–7], which includes the Bilong Co and Shengli River-Changshe Mountain oil shale zones. These zones potentially represent the largest marine oil shale resource in China.

The Bilong Co oil shale zone is also of special interest because the organic geochemistry of organic-rich oil shale can be correlated with that of the Early Toarcian anoxic event in Europe [8]. Earlier studies of oil shale were focused on organic geochemistry [9, 10] and anoxic event [8, 10]. However, little work has been done so far on the isotopic characteristics of oil shale, especially radiogenic isotopes. Knowledge of the characteristics of the Sr and Nd isotopes present in oil shale is very important, as it provides unique information about paleoenvironmental changes and detrital sediment sources along with the bulk chemistry and clay mineralogy of the sediment [11].

In the present study, Sr and Nd isotopic data for the Bilong Co oil shale from the Qiangtang basin, northern Tibet, China, were analyzed. The aim of the paper was to reconstruct paleoenvironmental changes, as recorded by the respective change in the Bilong Co oil shale section, and discuss sediment sources.

2. Geological setting

On a large scale, the Tibetan Plateau constitutes a tectonic collage of continental blocks. From north to south, Tibet is composed of the Kunlun-Qaidam area, the Songpan-Ganzi flysch complex, and the Qiangtang and Lhasa terranes, which are separated by the east-striking Anyimaqen-Kunlun-Muztagh, Hoh Xil-Jinsha River and Bangong Lake-Nujiang River suture zones, respectively (Fig. 1a). It is generally accepted that the Paleo-Tethys, represented by the Jinsha River suture zone, probably opened during the Early Carboniferous [12] and closed by the Permian to latest Triassic [13]. The mid-Tethys branch between the Lhasa and Qiangtang terranes was open by the Early Jurassic [13] and closed along the Bangong Lake-Nujiang River suture during the Late Jurassic [12].

Marked by the Hoh Xil-Jinsha River suture zone to the north and the Bangong Lake-Nujiang River suture zone to the south, the Qiangtang block consists of the North Qiangtang depression, the central uplift and the South Qiangtang depression (Fig. 1a) [14]. During the Permo-Trissic, the Paleo-Tethys Ocean was consumed by northern subduction beneath the Kunlun

terrane and southward subduction beneath the Qiangtang terrane [13], resulting in a large-scale regression in the Qiangtang basin. During this period, most parts of the Qiangtang basin were uplifted and exposed to erosion. Meanwhile paleo-weathering crusts occurred widely in the Qiangtang basin [15]. Subsequently, these weathering crusts were unconformably overlain by a succession of volcanic-volcaniclastic strata (the Late Triassic Nadi Kangri Formation volcanic-volcaniclastic rocks) that mark the onset of the Mesozoic Qiangtang basin [16]. As a result, the sediments are almost exclusively Mesozoic marine deposits that crop out in the South Qiangtang and North Qiangtang depressions, whereas Paleozoic marine sedimentary sequences are locally preserved in the central uplift.

The Bilong Co area is located in the South Qiangtang depression, northern Tibetan Plateau, China (Fig. 1b), where Jurassic marine strata are widespread, including the Lower Jurassic Quse Formation, the Middle Jurassic Sewa Formation, the Buqu and Xiali Formations, and the Upper Jurassic Suowa Formation (Fig. 1c). Oil shale, whose layer is about 35.5 m in thickness, is exposed for a distance of more than 4 km in the east-west direction. Abundant ammonites (*Harpoceras* sp.), occurring at the top of the Bilong Co oil shale section [9], indicate that the Bilong Co oil shale is of Early Jurassic age (i.e. Quse Formation strata).

The minerals identified by X-ray diffraction in oil shale include abundant calcite, clay minerals, quartz, minor dolomite, feldspars and pyrite [17]. Anhydrite and hematite have also been detected in several oil shale samples [17]. Clay minerals are common and occur in thin-layered and massive

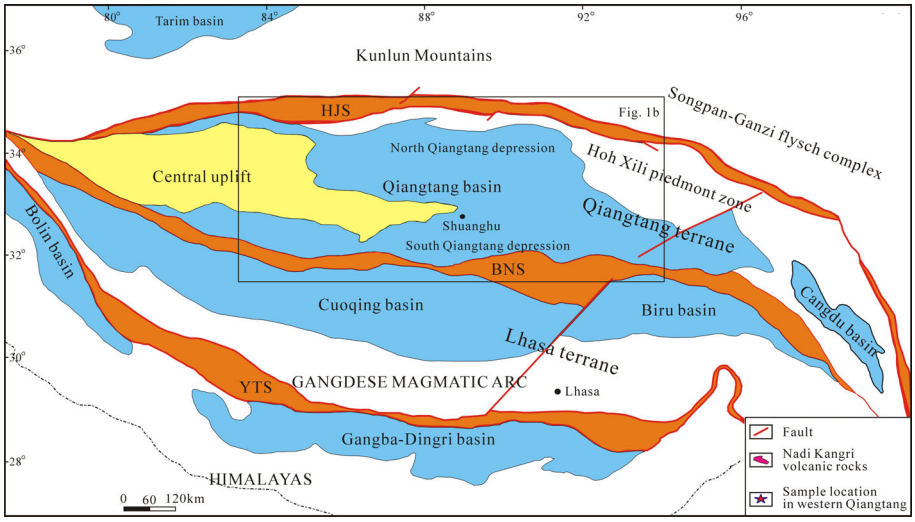

Fig. 1a. Map of the Tibetan Plateau showing major terranes [9].

HJS, Hoh Xil-Jinsha River suture; BNS, Bangong Lake-Nujiang River suture; YTS, Yarlung Tsangpo suture; HMLY, Himalayas.

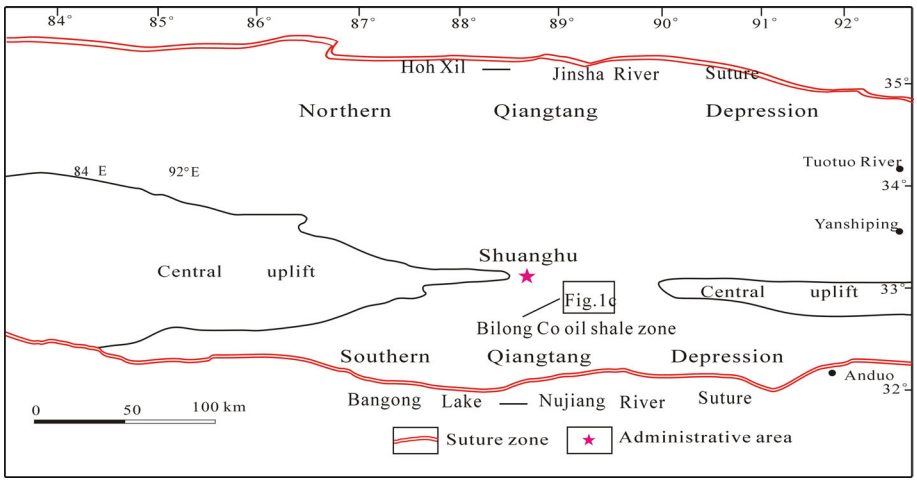

Fig. 1b. Generalized map showing the location of the study area.

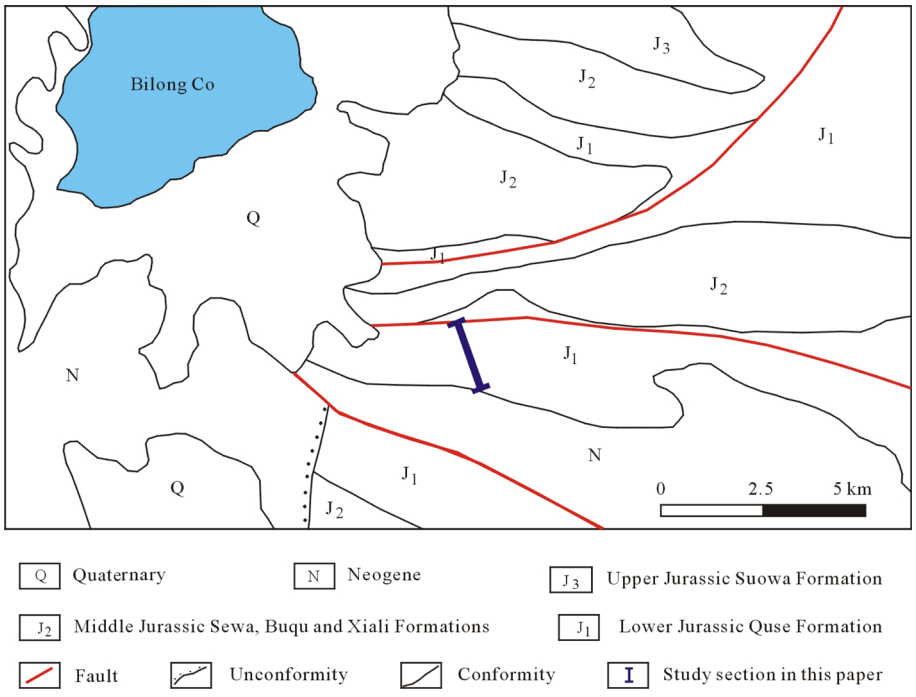

Fig. 1c. Simplified geological map of the Bilong Co area showing the location of the oil shale section.

forms. Calcite, whose content of the Bilong Co oil shale is high, occurs mainly as disseminated fine particles [17]. Quartz is mostly present as disseminated fine particles too. Pyrite is also found and occurs chiefly as disseminated fine particles. Minor quantities of pyrite crystals were detected in a field survey [17].

3. Samples and analytical methods

The location of the study area and oil shale section is shown in Figs. 1b and 1c, respectively. A total of 18 fresh unmetamorphosed samples were collected from the Bilong Co oil shale section. 13 samples were collected from oil shale seams with an average vertical sampling interval of 1 m, and five samples were taken from micritic limestone intervals.

Powdered samples (200 Mesh) were first heated to decompose organic materials prior to Sr-Nd isotopic analysis. The concentration of Sr isotopes was measured on a GV Isoprobe-T thermal ionization mass spectrometer (TIMS) at the Institute of Geology and Geophysics, Chinese Academy of Sciences. The analytical technique followed the procedure described by Ma *et al*. [18]. $^{88}Sr/^{86}Sr=0.1194$ was adopted to calibrate mass bias during measurements, and the NBS 987 Sr standard was repeatedly measured to monitor the quality of measurements, yielding an average $^{87}Sr/^{86}Sr$ of 0.710265±0.000009 (2σ) (N=24). Nd concentration measurements were carried out on a MicroMass Isoprobe multi-collector inductively coupled plasma mass spectrometer (MC-ICP-MS) at the Guangzhou Institute of Geochemistry, Chinese Academy of Sciences (GIG-CAS). The analytical procedures have been described by Liang *et al*. [19]. The fractionation of the measured $^{143}Nd/^{144}Nd$ was normalized using $^{146}Nd/^{144}Nd=0.7219$. A standard Nd solution, the Shin-Etsu JNDi-1, was repeatedly measured, yielding a mean value of 0.512118±0.000009 (2σ) (N=20) for $^{143}Nd/^{144}Nd$. The accuracy of measurement of concentrations and the Sm/Nd ratio was better than 2%.

4. Results

Isotopic data for oil shale and micritic limestone samples from the Bilong Co area are graphically presented as initial $^{87}Sr/^{86}Sr$ versus initial ε_{Nd} in Fig. 2 and tabulated in Table 1. The Sr and Nd isotopic ratios were age-corrected to the 183 Ma age based on the Early Toarcian ammonites [9].

Table 1. Sr and Nd isotope data for selected major and trace elements in Bilong Co oil shale and micritic limestone samples (Mn, Zr and ∑REE values from Ref. [17])

Sample site	Lithology	Rb, ppm	Sr, ppm	$^{87}Rb/^{86}Sr$	$^{87}Sr/^{86}Sr$	2ó	$^{87}Sr/^{86}Sr_i$	Sm, ppm	Nd, ppm	$^{147}Sm/^{144}Nd$	$^{143}Nd/^{144}Nd$	2ó	$^{143}Nd/^{144}Nd_i$	$\varepsilon_{Nd}(0)$	$\varepsilon_{Nd}(i)$	T_{DM}, Ga	Mn, %	Zr, ppm	∑REE, ppm
BP-6	Micritic limestone	87.6	309	0.7189	0.710061	0.000011	0.70819	2.35	12.5	0.1095	0.512053	0.000006	0.511922	-11.4	-9.4	1604	0.027	48.6	71.81
BP-7-1	Oil shale	79.2	338	0.5848	0.709619	0.000013	0.70810	2.07	11.9	0.1065	0.512053	0.000006	0.511925	-11.4	-9.3	1560	0.029	48.3	67.72
BP-7-2	Oil shale	74.9	345	0.5627	0.709512	0.000014	0.70805	1.95	11.2	0.1095	0.512066	0.000007	0.511935	-11.2	-9.1	1585	0.029	45.6	63.96
BP-7-3	Oil shale	72.8	318	0.5893	0.709682	0.000014	0.70815	2.05	11.2	0.1142	0.512064	0.000007	0.511927	-11.2	-9.3	1663	0.030	42.1	64.04
BP-8	Micritic limestone	72.9	413	0.4453	0.709410	0.000016	0.70825	1.86	10.4	0.1150	0.512041	0.000009	0.511903	-11.6	-9.7	1712	0.028	42.1	60.25
BP-9	Micritic limestone	34.3	505	0.1585	0.707875	0.000016	0.70746	1.19	5.83	0.1115	0.512028	0.000010	0.511894	-11.9	-9.9	1673	0.029	20.9	34.57
BP-10-1	Oil shale	83.9	343	0.6016	0.709896	0.000014	0.70833	2.86	15.2	0.1155	0.512063	0.000009	0.511925	-11.2	-9.3	1686	0.026	53.5	88.21
BP-10-2	Oil shale	93.6	600	0.3766	0.709049	0.000014	0.70807	2.68	15.2	0.1136	0.512041	0.000010	0.511905	-11.6	-9.7	1688	0.033	55.8	87.70
BP-10-3	Oil shale	96.1	457	0.5324	0.709653	0.000016	0.70827	3.61	16.6	0.1213	0.512054	0.000008	0.511909	-11.4	-9.6	1807	0.026	59.3	97.09
BP-10-4	Oil shale	127	381	0.8143	0.710875	0.000013	0.70876	3.87	20.4	0.1168	0.512053	0.000007	0.511913	-11.4	-9.5	1725	0.028	80.7	117.85
BP-11	Micritic limestone	22.9	639	0.0893	0.707536	0.000016	0.70730	0.93	4.65	0.1238	0.512047	0.000011	0.511899	-11.5	-9.8	1868	0.041	23.4	26.25
BP-12-1	Oil shale	81.5	442	0.4565	0.709221	0.000014	0.70803	2.99	14.6	0.1217	0.512054	0.000009	0.511908	-11.4	-9.6	1814	0.031	55.6	85.32
BP-12-2	Oil shale	83.6	491	0.4322	0.709158	0.000016	0.70803	2.61	13.5	0.1190	0.512008	0.000010	0.511865	-12.3	-10.5	1836	0.029	55.8	80.58
BP-12-3	Oil shale	112	476	0.5937	0.709855	0.000013	0.70831	3.77	19.3	0.1131	0.512027	0.000008	0.511892	-11.9	-10.0	1701	0.033	76.3	112.21
BP-13	Micritic limestone	25.2	415	0.1594	0.707902	0.000014	0.70749	1.33	6.41	0.1216	0.512026	0.000009	0.511880	-11.9	-10.2	1858	0.067	25.8	36.14
BP-14-1	Oil shale	75.3	449	0.4322	0.709273	0.000014	0.70815	3.04	15.5	0.1121	0.512045	0.000006	0.511911	-11.6	-9.6	1657	0.029	53.3	87.60
BP-14-2	Oil shale	79.3	434	0.4814	0.709237	0.000013	0.70798	2.96	15.2	0.1211	0.512073	0.000007	0.511928	-11.0	-9.3	1772	0.036	51.2	84.40
BP-14-3	Oil shale	71.5	472	0.3741	0.708800	0.000011	0.70783	2.96	14.8	0.1249	0.512067	0.000007	0.511917	-11.1	-9.5	1857	0.026	51.7	83.41

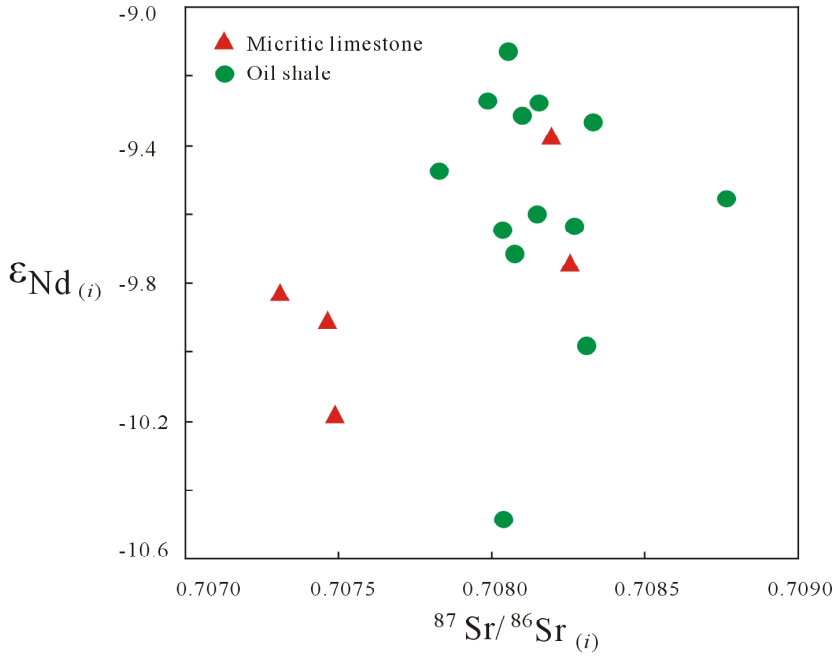

Fig. 2. $^{87}Sr/^{86}Sr_{(i)}$ vs. $\varepsilon_{Nd(i)}$ values for the samples under study.

4.1. Sr isotopes

Our results (Table 1) show that the Sr concentrations of oil shale samples exceeded 318 ppm, with a maximum of 600 ppm and an average of 427 ppm. In contrast, micritic limestone samples had a higher Sr concentration varying between 309 and 639 ppm, with an average of 456 ppm. All samples had a low Rb/Sr ratio ranging from 0.04 to 0.33. The $^{87}Sr/^{86}Sr$ ratios of samples cluster into discrete groups with minimal overlap: 0.70783–0.70876 for the oil shale group, and 0.70730–0.70825 for the micritic limestone group (Fig. 2). Overall, the Sr isotopic ratios rapidly decrease upwards from oil shale seams to micritic limestone intervals.

4.2. Nd isotopes

In the oil shale samples from the Bilong Co area the concentrations of Sm and Nd ranged from 0.93 to 3.87 ppm and from 4.65 to 20.4 ppm, respectively, while the Sm/Nd ratio varied only a little, $^{147}Sm/^{144}Nd$ remaining between 0.1065 and 0.1249. The measured values of $\varepsilon_{Nd}(0)$ varied from –12.3 to –11.0. The Nd isotopic composition of samples revealed no obvious systematic change with increasing stratigraphic height (Fig. 3).

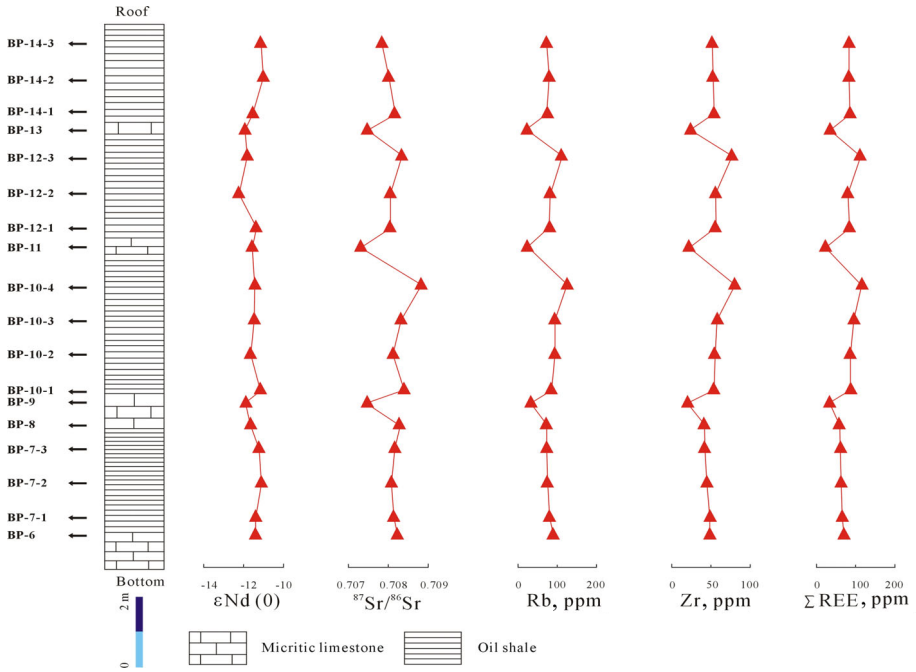

Fig. 3. Vertical variations of $\varepsilon_{Nd}(0)$, Sr isotope, ∑REE and selected trace elements in the Bilong Co oil shale section. Note a small fluctuation of $\varepsilon_{Nd}(0)$ through the section, and a consistent pattern between the $^{87}Sr/^{86}Sr$ ratio and concentrations of Zr, Rb and ∑REE.

5. Interpretation and discussion

5.1. Mode of occurrence of Rb, Sr, Sm and Nd

In general, elements in oil shale occur in combination with either organic or inorganic constituents. Inorganic constituents may comprise more than one component with distinct elemental signatures. The mode of occurrence of elements in oil shale can be inferred from its association with particular minerals or major elements, based on Pearson's correlation coefficients between the elements. Coarse-grained detrital minerals are rare in the Bilong Co oil shale. The absorption of fine-grained minerals and/or organic matter may be the main mode of occurrence of Rb, Sr, Sm and Nd. It is to be noted that the concentrations of Rb, Sm, and Nd positively correlated with ash yield [17], which shows that detrital minerals in oil shale are the main carriers of these elements. The prevailingly positive correlations between the concentrations of Si and Rb (r = 0.97), Sm (r = 0.78) and Nd (r = 0.85), Al and Rb (r = 0.98), and Sm (r = 0.83) and Nd (r = 0.91) imply that Rb, Sm, and Nd are mainly present in clay minerals.

The concentration of strontium only slightly correlated with ash yield [17], suggesting that Sr is different in mode of occurrence from the other elements under study.

5.2. Use of Nd isotope data in source determination

Nd isotopes can provide important information about the provenance of clastic sediments in marine environments [20]. The present-day values of $\varepsilon_{Nd}(0)$ and the $^{147}Sm/^{144}Nd$ ratio of oil shale are relatively uniform, with small variations between –12.3 and –11.0, and 0.1065 and 0.1249, respectively. The Sm-Nd model ages (or crustal residence ages) are restricted to a range of 1.56–1.86 Ga (Table 1). The depositional age of the Bilong Co oil shale is about 183 Ma [7]. The obtained data suggest that the shale is of Meso-/Paleoproterozoic origin. However, the Bilong Co oil shale was deposited in the Early Toarcian coincident with the peak of the Early Jurassic transgression [7]. Sedimentary facies and palaeogeographic reconstruction reveal that potential sources (or sediment supply areas) for oil shale are located in the southern part of the central uplift [14] where the Mesozoic strata are widely spread, including the Late Triassic Nadi Kangri Formation volcanic-volcaniclastic rocks and conglomerates. Additionally, the gravel components of Nadi Kangri Formation conglomerates mainly consist of Nadi Kangri Formation volcanic gravels and underlying limestone [14]. These data rule out the Meso-/Paleoproterozoic sediments as major source rocks for the Bilong Co oil shale. The values of the $^{147}Sm/^{144}Nd$ ratio of oil shale samples reported here are similar to those of the Late Triassic Nadi Kangri Formation rhyolite (average 0.1267) and tuff (average 0.1076) (Table 2), indicating that the shale originates from the Nadi Kangri Formation volcanic-volcaniclastic rocks. Moreover, our results reveal that the difference in average $\varepsilon_{Nd}(0)$ between oil shale samples and the Nadi Kangri Formation volcanic-volcaniclastic rocks is only 0.6ε (Table 2), which further supports the above recognition. The Sm-Nd model ages for oil shale samples also second the shale's derivation from the Nadi Kangra source whose model ages reflect the

Table 2. Nd isotopic data for oil shales and Nadi Kangri Formation volcanic-volcaniclastic rocks

Sediment	$^{147}Sm/^{144}Nd$	$^{143}Nd/^{144}Nd$	$\varepsilon_{Nd}(0)$
Samples from the Bilong Co oil shale profile			
Oil shale	0.1065–0.1249 (average 0.1161)	0.511865–0.511935 (average 0.511912)	–12.3 to –11.0 (average –11.4)
Micritic limestone	0.1095–0.1238 (average 0.1163)	0.511880–0.511922 (average 0.511900)	–11.9 to –11.4 (average –11.7)
Nadi Kangri Formation volcanic-volcaniclastic rocks			
Rhyolite	0.1203–0.2566 (average 0.1267)	0.511789–0.511886 (average 0.511845)	–12.7 to –11.2 (average –12.0)
Tuff	0.1064–0.1088 (average 0.1076)	0.511868–0.511886 (average 0.511877)	–12.2 to –11.6 (average –11.9)

stemming of volcanic rocks from the older continental crust by its melting. The model ages of the Bilong Co oil shale are similar to those of the Nadi Kangri Formation rhyolite (~1.7–1.9 Ga), tuff (~1.6–1.7 Ga) and granite (~1.7–2.0 Ga).

5.3. Stability of source regions across the oil shale profile

The change in Nd isotopes concentration could be attributed to the change of sediment provenance [21]. Table 1 shows that the $\varepsilon_{Nd}(0)$ values in the Bilong Co oil shale profile range from –12.3 to –11.0, with an average of –11.5. The respective values of oil shale seams vary between –12.3 and –11.0, with an average of –11.4, whereas those for micritic limestone intervals remain between –11.9 and –11.4, with an average of –11.7. The difference in averages between oil shale seams and micritic limestone intervals is only 0.3ε unit. This is indicative of the relatively homogeneous $\varepsilon_{Nd}(0)$ values in the whole profile, as well as of the comparatively stable provenance of oil shale and micritic limestone in the Bilong Co oil shale profile.

As seen from Fig. 3, the fluctuations of $\varepsilon_{Nd}(0)$ values in the Bilong Co oil shale profile are small. The respective maximum fluctuations from micritic limestone beds to oil shale seams are observed at the boundary between BP-9 and BP-10-1, the variations being smaller than 0.7ε unit. Wang *et al.* proposed that the total experimental error of $^{143}Nd/^{144}Nd$ is generally accepted to be within ±0.000050, which would lead to a change of $\varepsilon_{Nd}(0)$ not beyond 0.7ε unit [22]. Thus, the Nd isotopic composition has changed or an isotopic anomaly takes place only when the difference in $\varepsilon_{Nd}(0)$ values between the samples is larger than $0.7\varepsilon_{Nd}$ unit [22]. Obviously, a smaller fluctuation of $\varepsilon_{Nd}(0)$ than 0.7ε unit from micritic limestone beds to oil shale seams indicates that the source regions of micritic limestone cannot be shown to be different from those of oil shale.

5.4. Sr isotope evidence for sources of oil shale

The $^{87}Sr/^{86}Sr$ ratio varies between 0.70730 and 0.70876. The isotopes of Sr are not fractionated in nature. Thus, during deposition the Bilong Co oil shale may record the isotopic compositions of Sr in the latest Early Jurassic seawater and/or sediment source. Our study revealed that all oil shale samples had a higher $^{87}Sr/^{86}Sr$ ratio than contemporary seawater. This can be explained by the following. The Bilong Co oil shale was either diagenetically altered due to addition of radiogenic Sr after their precipitation, or the precipitation fluid had a high $^{87}Sr/^{86}Sr$ ratio. The analysis of Mn and Sr concentrations, as well as values of their ratio has become an effective tool in evaluating the intensity of diagenetic alterations [23]. The Bilong Co oil shale is characterized by a low concentration of Mn and a very low ratio of Mn/Sr (0.54–0.95). Furthermore, there is no correlation between the $^{87}Sr/^{86}Sr$ ratio and Mn concentration (Fig. 4). Some samples of oil shale, whose Mn concentration is high, possess a low $^{87}Sr/^{86}Sr$ ratio. This implies that dia-

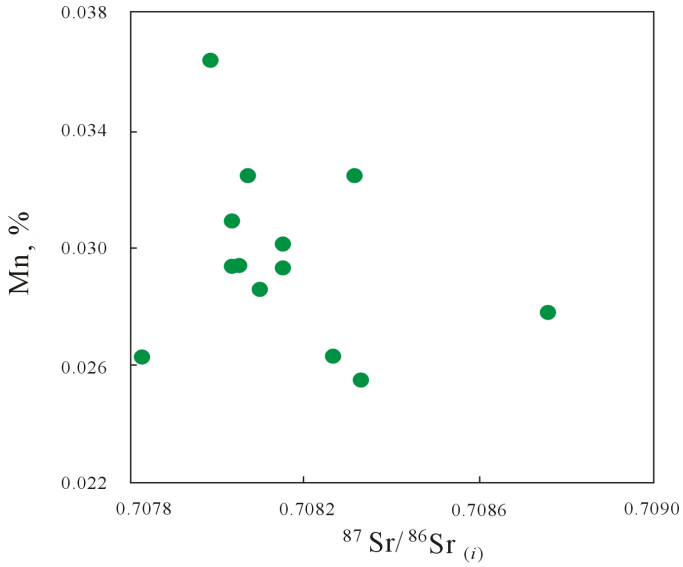

Fig. 4. Relationship between the $^{87}Sr/^{86}Sr$ ratio and Mn content of Bilong Co oil shale samples (Mn value from Ref. [17]).

genesis has a negligible impact on $^{87}Sr/^{86}Sr$ values. Consequently, the high $^{87}Sr/^{86}Sr$ ratio of the Bilong Co oil shale reflects the original composition of the deposited sediment, both chemical and clastic.

The high $^{87}Sr/^{86}Sr$ ratio of Bilong Co oil shale samples suggests that radiogenic ^{87}Sr had a significant input to the Sr system during deposition. Such a high $^{87}Sr/^{86}Sr$ ratio is indicative of a radiogenic strontium flux and the shale's $^{87}Sr/^{86}Sr$ ratio was derived from tectonoclimatic processes such as the exposure and chemical weathering of ancient crystalline rocks with high $^{87}Sr/^{86}Sr$ ratio [24]. Our study of Nadi Kangri Formation strata reveals that the average Sr content of the exposed Nadi Kangri Formation rhyolite and tuff is 122.4 and 104.8 ppm, respectively. Both the rocks have a high $^{87}Sr/^{86}Sr$ ratio, i.e. about 0.7090 and 0.7118, respectively. Thus, the radiogenic strontium, which is responsible for the high $^{87}Sr/^{86}Sr$ ratio of oil shale, was probably derived from the Nadi Kangri volcanic-volcaniclastic rocks. The significantly positive correlations between the $^{87}Sr/^{86}Sr$ ratio and contents of Si (statistically significant at a strict significance level of 0.001; the linear correlation coefficient r=0.88) and Al (r=0.84) further imply that weathering clay minerals with more radiogenic Sr may have an important role in the detrital input to oil shale.

5.5. Sr isotopic change and sea level fluctuations

In the Bilong Co oil shale area, micritic limestone generally has a slightly lower $^{87}Sr/^{86}Sr$ ratio than oil shale. At Site BP-12-3, the oil shale's $^{87}Sr/^{86}Sr$ ratio is 0.70831, whereas that of micritic limestone is 0.70749 at Site BP-13, indicating a dramatic shift in Sr isotope concentration at the boundary

between oil shale seams and micritic limestone beds. A similar shift in SR isotope concentration is also observed at sites BP-10-4 to BP-11 (Fig. 3). The Sr concentration of the samples of both sediments is high, being respectively 413–639 and 318–600 ppm, while their Mn/Sr ratio is low, 0.57–1.62 and 0.54–0.95, respectively. This excludes diagenetic alteration as a factor which is responsible for the decrease in $^{87}Sr/^{86}Sr$ ratio from oil shale seams to micritic limestone intervals. This decrease may be accounted for: (1) a change in oceanic circulation pattern, (2) a change in Sr isotope concentration of local or regional continental inputs, and (3) a compositional change of the precipitation fluid.

As discussed above, the vertical variations of $\varepsilon_{Nd}(0)$ values in the Bilong Co oil shale section are relatively homogeneous, which is indicative of a stable provenance of sediments with no significant change of source regions from the oil shale seam to the micritic limestone bed. The decreases upwards from oil shale to micritic limestone suggest that the clastic content is a critical factor. It is to be noted that the $^{87}Sr/^{86}Sr$ ratio reveals a consistent vertical variation with Zr, Rb, and ∑REE distributions (Fig. 3) and has a highly positive relationship with the contents of Zr, Rb, and ∑REE (Fig. 5). These data further support the above observations.

Influenced by regional tectonics, sea level fluctuations in the Qiangtang basin were frequent during the Early Jurassic. When the relative sea level was low, a barrier-lagoon system was formed in the Bilong Co area. As a result, the area was isolated from the sea by a paleotopographic high barrier. Subsequently, a wide lagoonal area developed behind the protecting barriers. Oil shale was mainly deposited in the lagoonal environment. Therefore, the shale's high $^{87}Sr/^{86}Sr$ ratio is chiefly controlled by weathering clay minerals with more radiogenic Sr. However, when the relative sea level was high; the barriers were submerged as they continued to undergo transgression, resulting in open-ocean environments in the Bilong Co area. Sea level rise and consequent marine incursion may have changed the aquatic environment of the pre-existing lagoon, ending the deposition of oil shale. Furthermore, introduction of seawater Sr would lower the precipitation fluid's $^{87}Sr/^{86}Sr$ ratio. Frequent sea level changes responded to repetitive cycles of oil shale and micritic limestone depositions, resulting in Sr isotope concentration fluctuation from oil shale seams to micritic limestone intervals.

Frimmel speculated that trace element distributions in carbonates can be useful monitors of the depositional palaeoenvironment. The low contents of Zr, Rb and ∑REE (total rare earth element) reflect a distal depositional environment, whereas the high ones are probably related to deposition in a near-shore environment [25]. The Bilong Co oil shale has relatively high concentrations of Zr (average 56.1 ppm), Rb (average 87.0 ppm) and ∑REE (average 86.2 ppm) (Fig. 3), which is in agreement with deposition in the near-shore environment (lagoon). In contrast, the concentrations of Zr (average 32.2 ppm), Rb (average 48.6 ppm) and ∑REE (average 45.8 ppm) of micritic limestone are lower (Fig. 3), reflecting deposition in the open-ocean environment.

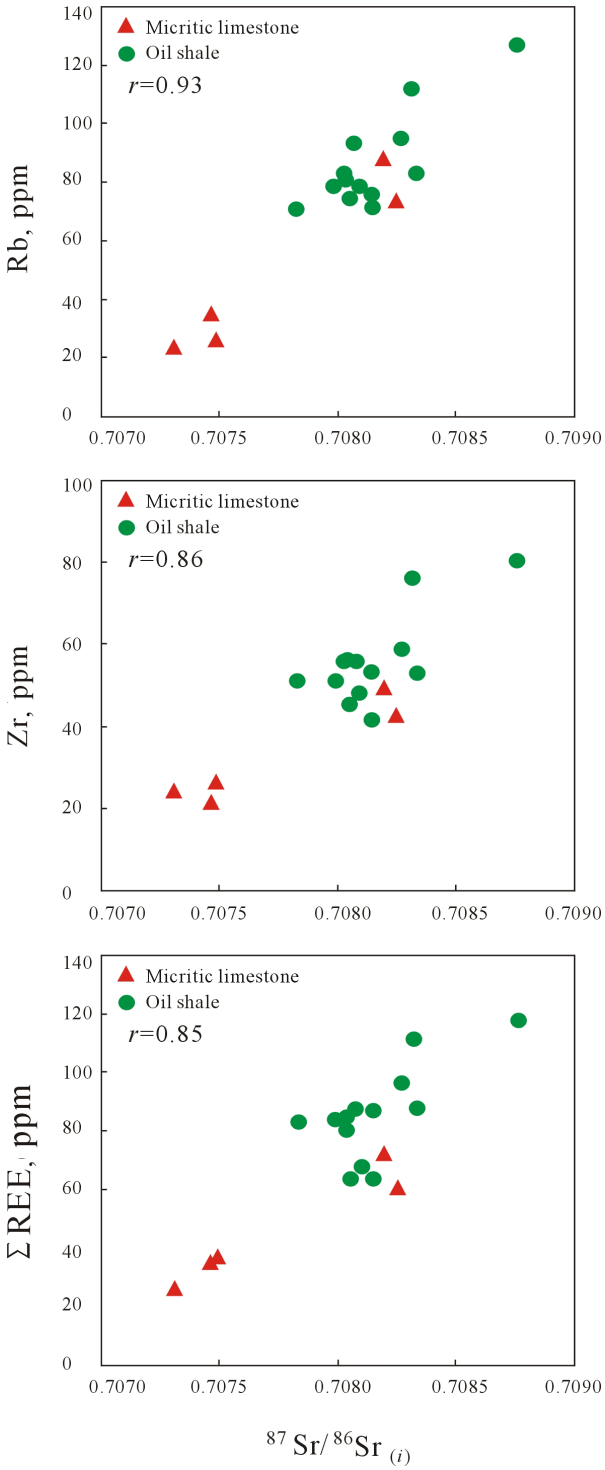

Fig. 5. Relationship between the $^{87}Sr/^{86}Sr$ ratio and contents of Rb, Zr, and ∑REE of Bilong Co oil shale samples (Zr and ∑REE values from Ref. [17]).

6. Conclusions

(1) The Nd isotopic composition of oil shale samples from the Bilong Co area is similar to that of the Late Triassic Nadi Kangri Formation volcanic-volcaniclastic rocks, implying that the shale originates from the Nadi Kangri Formation volcanic-volcaniclastic rocks. The Sm-Nd model ages for oil shale samples also support its derivation from the Nadi Kangri source whose model ages reflect the origin of volcanic rocks from the older continental crust by its melting.

(2) The vertical variations of $\varepsilon_{Nd}(0)$ values in the Bilong Co oil shale section are relatively homogeneous, indicating a stable provenance of sediments with no significant change of source regions from the oil shale seam through the micritic limestone bed.

(3) The $^{87}Sr/^{86}Sr$ ratio of Bilong Co oil shale samples ranges from 0.70783 to 0.70876, being much higher than that of contemporary seawater. Such a high $^{87}Sr/^{86}Sr$ ratio reflects the original composition of the deposited sediment, both chemical and clastic. The radiogenic strontium, which is responsible for the high $^{87}Sr/^{86}Sr$ ratio of oil shale samples, was probably derived from the Nadi Kangri volcanic-volcaniclastic rocks.

(4) The Bilong Co oil shale was deposited in the lagoonal environment. Sea level rise and consequent marine incursion may change the aquatic environment of the pre-existing lagoon, lowering the precipitation-fluid's $^{87}Sr/^{86}Sr$ ratio. Frequent regional sea level changes would result in Sr isotope concentration fluctuation from oil shale seams to micritic limestone intervals.

Acknowledgements

This work was supported by the National Natural Science Foundation of China (Grants 41172098, 40972087), the Sichuan Youth Science & Technology Foundation (No. 09ZQ026-006), and the National Oil and Gas Special Project (No. XQ-2009-01).

REFERENCES

1. Qian, J. L. China's oil business is going ahead. *Oil Shale*, 2006, **23**(4), 295.
2. Liu, Z. J., Yang, H. L., Dong, Q. S., Zhu, J. W., Guo, W., Ye, S. Q., Liu, R., Meng, Q. T., Zhang, H. L., Gan, S. C. *Oil shale in China*. Petroleum Industry Press, Beijing, 2009, 157–167 (in Chinese with English abstract).
3. Qian, J. L., Yin, L., Wang, J. Q., Li, S. Y., Han, F., He, Y. G. *Oil shale – a supplementary energy of petroleum*. China Petrochemical Press, Beijing, 2008, 23 (in Chinese).
4. Wang, C. S., Zhang, S. M. The discovery of oil shale in the Shuanghu area, northern Tibet, China. *Geology in China*, 1987, 8, 29–31 (in Chinese).

5. Fu, X. G., Wang, J., Qu, W. J., Duan, T. Z., Du, A. D., Wang, Z. J., Liu, H. Re-Os (ICP-MS) dating of marine oil shale in the Qiangtang basin, northern Tibet, China. *Oil Shale*, 2008, **25**(1), 47–55.
6. Fu, X. G., Wang, J., Zeng, Y. H., Li, Z. X., Wang, Z. J. Geochemical and palynological investigation of the Shengli River marine oil shale (China): Implications for paleoenvironment and paleoclimate. *Int. J. Coal Geol*., 2009, **78**(3), 217–224.
7. Fu, X. G., Wang, J., Zeng, Y. H., Chen, J., Tan, F. W. Origin and mode of occurrence of trace elements in marine oil shale from the Shengli River area, northern Tibet, China. *Oil Shale*, 2011, **28**(4), 487–506.
8. Chen, L., Yi, H. S., Hu, R. Z., Zhong, H., Zou, Y. R. Organic geochemistry of the Early Jurassic oil shale from the Shuanghu area in northern Tibet and the Early Toarcian oceanic anoxic event. *Acta Geol. Sin-Engl.*, 2005, **79(**3), 392–397.
9. Lin, J. H., Yi, H. S., Li, Y., Wang, C. S., Peng, P. A. Characteristics of bio-marker compounds and its implication of Middle Jurassic oil shale sequence in Shuanghu area, northern Tibetan Plateau. *Acta Sedimentologica Sinica*, 2001, **19**(2), 287–292 (in Chinese with English abstract).
10. Yi, H. S., Deng, B., Xiong, S. P. Lower Jurassic oil shale deposition from northern Tibet: chemostratigraphic signals and the early Toarcian anoxic event. In: *18th HKT Workshop Abstracts*, 2003, 129–130.
11. Weldeab, S., Siebel, W., Wehausen, R., Emeis, K.-C., Schmiedl, G., Hemleben, C. Late Pleistocene sedimentation in the Western Mediterranean Sea: Implications for productivity changes and climatic conditions in the catchment areas. *Palaeogeogr. Palaeocl.,* 2003, **190**(3-4), 121–137.
12. Yin, A., Harrison, T. M. Geologic evolution of the Himalayan-Tibetan Orogen. *Annu. Rev. Earth Pl. Sc.,* 2000, **28**, 211–280.
13. Kapp, P., Yin, A., Manning, C. E., Harrison, T. M., Taylor, M. H., Ding, L. Tectonic evolution of the early Mesozoic blueschist-bearing Qiangtang metermorphic belt, central Tibet. *Tectonics*, 2003, **22**(4), 1043.
14. Wang, J., Ding, J., Wang, C. S., Tan, F. W., Chen, M., Hu, P., Li, Y. L., Gao, R., Fang, H., Zhu, L. D., Li, Q. S., Zhang, M. H., Du, B. W., Fu, X. G., Li, Z. X., Wan, F. *Survey and evaluation on Tibet oil and gas resources*. Geological Publishing House, Beijing, 2009, 6 (in Chinese).
15. Fu, X. G., Wang, J., Zeng, Y. H., Tan, F. W., Feng, X. L. REE Geochemistry of marine oil shale from the Changshe Mountain area, northern Tibet, China. *Int. J. Coal Geol*., 2010, **81**(3), 191–199.
16. Fu, X. G., Wang, J., Tan, F. W., Chen, M., Chen, W. B. The Late Triassic rift-related volcanic rocks from eastern Qiangtang, northern Tibet (China): Age and tectonic implications. *Gondwana Res*., 2010, **17**(1), 135–144.
17. Fu, X. G., Wang, J., Zeng, Y. H., Tan, F. W., Feng, X. L. Concentration and mode of occurrence of trace elements in marine oil shale from the Bilong Co area, northern Tibet, China. *Int. J. Coal Geol*., 2011, **85**(1), 112–122.
18. Ma, J. L., Wei, G. J., Xu, Y. G., Long, W. G. Variations of Sr− Nd− Hf isotopic systematics in basalt during intensive weathering. *Chem. Geol*., 2010, **269**(3-4), 376–385.
19. Liang, X. R., Wei, G. J., Li, X. H., Liu, Y. Precise measurement of $^{143}Nd/^{144}Nd$ and Sm/Nd ratios using multiple-collectors inductively coupled plasma-mass spectrometry (MC-ICPMS). *Geochimica*, 2003, **32**(1), 91–96 (in Chinese with English abstract).

20. Farmer, G. L., Ball, T. T. Sources of Middle Proterozoic to Early Cambrian siliciclastic sedimentary rocks in the Great Basin: A Nd isotope study. *Bull. Geol. Soc. Am.*, 1997, **109**(9), 1193–1205.
21. Boulay, S., Colin, C., Trentesaux, A., Frank, N., Liu, Z. Sediment sources and East Asian monsoon intensity over the last 450 ky. Mineralogical and geochemical investigations on South China Sea sediments. *Palaeogeogr. Palaeocl.*, 2005, **228**(3-4), 260–277.
22. Wang, Y. X., Yang, J. D., Chen, J., Zhang, K. J., Rao, W. B. The Sr and Nd isotopic variations of the Chinese Loess Plateau during the past 7 Ma: Implications for the East Asian winter monsoon and source areas of loess. *Palaeogeogr. Palaeocl.*, 2007, **249**(3-4), 351–361.
23. Huang, S. J., Qing, H. R, Huang, P. P., Hu, Z. W., Wang, Q. D., Zou, M. L., Liu, H. N. Evolution of strontium isotopic composition of seawater from Late Permian to Early Triassic based on study of marine carbonates, Zhongliang Mountain, Chongqing, China. *Sci. China Ser. D,* 2008, **51**(4), 528–539.
24. Armstrong-Altrin, J. S., Lee, Y. I., Verma, S. P., Worden, R. H. Carbon, oxygen, and strontium isotope geochemistry of carbonate rocks of the upper Miocene Kudankulam Formation, southern India: Implications for paleoenvironment and diagenesis. *Chem. Erde-Geochem*., 2009, **69**(1), 45–60.
25. Frimmel, H. E. Trace element distribution in Neoproterozoic carbonates as palaeoenvironmental indicator. *Chem. Geol*. 2009, **258**(3-4), 338–353.

Presented by J. Boak
Received January 18, 2012